# Anomalous angular distributions in pion and $\alpha$ particle scattering to the $2_2^+$ state of $^{52}$Cr

D. S. Oakley
*Colorado Christian University, Lakewood, Colorado 80226*

R. J. Peterson
*Nuclear Physics Laboratory, University of Colorado, Boulder, Colorado 80309*

C. L. Morris
*Los Alamos National Laboratory, Los Alamos, New Mexico 87545*

H. T. Fortune
*University of Pennsylvania, Philadelphia, Pennsylvania 19104*

(Received 12 September 1995)

Inelastic scattering of 180 MeV $\pi^+$ and $\pi^-$ from $^{52}$Cr shows an angular distribution for the $2_2^+$ state at 2.96 MeV that differs greatly from the usual $L = 2$ shapes for $2^+$ states. This state is perhaps the only case from pion-inelastic scattering in which standard distorted-wave impulse approximation models (including multistep and single-step responses) fail to reproduce the measured angular distribution. Furthermore, this unique excitation has been shown to have the features expected of a seniority-four proton excitation yet the pion data show charge symmetry. While coupled-channel calculations are not able to reproduce the pion data, they do agree with the shape observed for 42 MeV $\alpha$ particle scattering to this state, but the magnitude of the $\alpha$ scattering data is not consistent with a collective model and known $\gamma$ ray deexcitations. Scattering to the first and third $2^+$ states of $^{52}$Cr with pions and $\alpha$ particles is also considered, and found to match the usual result for $2^+$ states in general, accentuating the anomaly of this $2_2^+$ transition.

PACS number(s): 27.40.+z, 24.10.Eq, 25.80.Ek

## I. INTRODUCTION

Inelastic pion scattering at beam energies corresponding to the delta resonance has been shown to give diffractive angular distributions characteristic of the orbital-angular momentum transfer to natural-parity states, and to give transition matrix elements for protons, neutrons, and their isoscalar sums and isovector differences in good accordance with other measurements [1]. A striking exception was found for 180 MeV pion scattering to the second $2^+$ state of $^{52}$Cr, at 2.96 MeV [2]. This has previously been shown to be of a very simple shell-model structure, based on the assumption of four valence $f_{7/2}$ protons excited from the ground state of seniority, $v = 0$, to a state of $v = 4$ [3,4]. Here, seniority is the number of unpaired nucleons outside doubly closed $^{48}$Ca. More recent electromagnetic data confirm that only a very weak electric quadrupole transition connects this state to the ground state, as expected if a change of four units of seniority is required [5,6]. A high-resolution electron scattering experiment also failed to excite this 2.96 MeV state [7].

Pion scattering to such a seniority-4 state would be very similar in its tensorial rank to pion double charge exchange (DCX), requiring explicit double excitation. The proton seniority 4, with inert neutrons, would lead to the expectation of a strong asymmetry between scattering $\pi^+$ and $\pi^-$. We here test this assumption against new scattering data, using first-order and second-order distorted-wave impulse approximation (DWIA) methods. The general expectations from the scattering of strongly absorbed spin-zero projectiles also permit a simple parametrization in terms of a diffraction model.

Inelastic scattering of $\alpha$ particles parallels that of pions as both involve strongly absorbed spin-zero projectiles. We apply the reaction models and the parameters found from analysis of the pion data to older $\alpha$ particle data to the same $2^+$ states for comparison. The $\alpha$ particle data ensure the correct choice of the relative phase for neutron and proton excitations by $\pi^+$ and $\pi^-$.

## II. PION SCATTERING

The new pion-scattering experiment was carried out with the EPICS system at LAMPF in order to improve upon the experiment described in [2], using a natural Cr target (83.8% $^{52}$Cr) and a beam energy of 180 MeV. The resolution attained was improved to 135 keV [full width at half maximum (FWHM)], counting statistics were increased, and backgrounds due to secondary elastic scattering were eliminated to obtain cleaner spectra in the region near 3 MeV of excitation [8]. The cross section scale was normalized, as in [2], to known $\pi^\pm$ proton and $\pi^\pm$ carbon elastic cross sections. Peak areas were extracted from the pion energy-loss spectra, with a peak shape derived from the elastic scattering peak, where the energy separations of the various states were constrained by known $^{52}$Cr excitation energies [5,6].

A potential source of background is from other Cr isotopes. In the even Cr isotopes, electron scattering [7] finds an $L = 2$ transition to a state of $^{50}$Cr at 2.92 MeV, which can not be resolved from the 2.96 MeV state. This should, however, produce $L = 2$ cross sections from pion scattering equivalent to no more than 11 $\mu$b/sr at forward angles, which is less than 10% of the 2.96 MeV strength observed in the present work. Several states of $^{53}$Cr could be in the 2.96 MeV peak

 

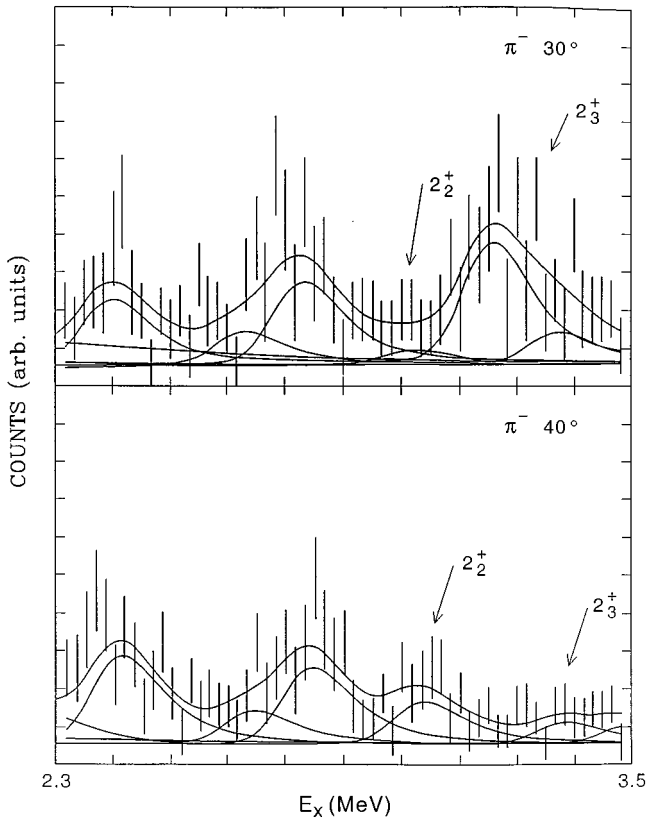


FIG. 1. Sample spectra for 180 MeV $\pi^-$ scattered from natural chromium. The top spectrum is at 30°, where standard $2^+$ transitions have a maximum, while the lower spectrum is at 40°, where $2^+$ states should have a minimum. The 2.96 MeV $2_2^+$ state is clearly out of phase with these expectations (unlike the $2_3^+$ state which is in phase).

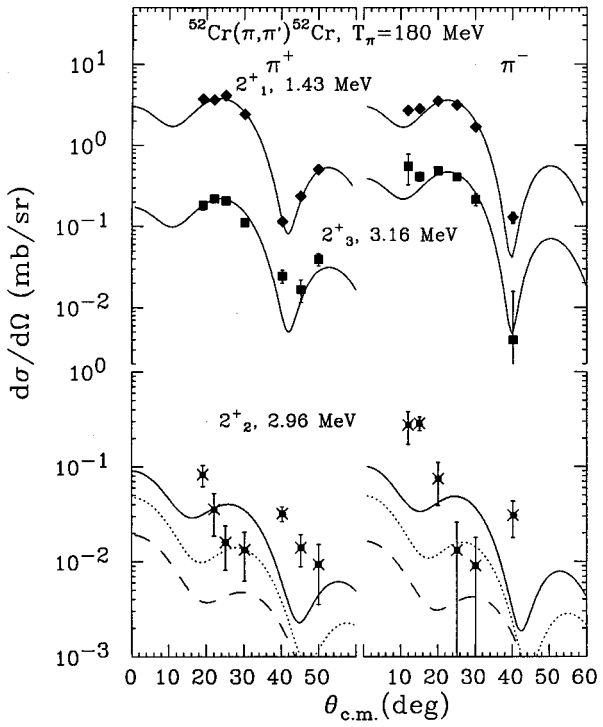


FIG. 2. Differential cross sections for the first, second, and third $2^+$ states of $^{52}$Cr are compared to first- and second-order DWIA calculations. The first-order curves for the 1.43 MeV (diamond data points) and 3.16 MeV (square points) transitions use the proton and neutron matrix elements listed in Table I. The solid curves for the 2.96 MeV data (crosses) use the first- and second-order paths, with matrix elements listed in Table I. The dotted curves use only the sequential two-step path through the first $2^+$ state, while the dashed curves show the result of taking the opposite relative sign for the first- and second-order amplitudes.

analyzed here [9], but they are of high multipolarity and weakly excited in low-energy proton scattering [10] in spite of their high statistical weight. The cross sections seen in the present work do not have the shapes expected for high multipolarity. We can conclude from these results on the other Cr isotopes in the natural target used here that the 2.96 MeV data presented here do indeed result from the population of the $2_2^+$ state of $^{52}$Cr.

Sample spectra are presented in Fig. 1. The top spectrum represents an angle corresponding to a diffractive $L=2$ maximum while the bottom is at an $L=2$ minimum. The 2.96 MeV peak, although weak, clearly does not show the same diffraction pattern found for the other $2^+$ states in $^{52}$Cr [2].

Differential cross sections for the first, second, and third $2^+$ states of $^{52}$Cr are presented in Fig. 2, with an overall normalization uncertainly of $\pm$ 8%. The $2_1^+$ cross sections agree with those of Ref. [2]. The solid curves represent the DWIA fits [11,12] to the 1.43 and 3.16 MeV data. The Kisslinger optical model is the basis of the DWIA calculations with $\pi$-nucleon amplitudes taken from [13]. Coupled-channels calculations were also performed to include impulse approximation scattering beyond first order [11]. In first order, this is just the DWIA familiar from the many results summarized in [1]. No back coupling of the transition strength was included in our calculations to keep the results for the elastic and first order transitions in concordance with the usage of first-order codes. An energy shift of $-28$ MeV was used, as in [2]. The geometrical parameters for the two-parameter Fermi distributions of neutrons and protons were kept the same, with $c=3.98$ fm and $a=0.48$ fm. Inelastic scattering was computed through the vibrational collective model, with a transition density proportional to the derivative of the ground-state distribution. Our model for the shell-model excitation is that of $f_{7/2}$ nucleons recoupled to states of seniority other than zero as found in the ground state. A transition density for this model is taken from calculations of a proton bound in a Woods-Saxon potential appropriate to $^{52}$Cr, as in Ref. [14]. Figure 3 compares the collective and microscopic proton model transition densities, both normalized to give $B(C2)\uparrow=672e^2$ fm$^4$. These are similar enough to justify our use of the simple derivative collective model for our reaction calculation. In the collective model one uses a deformation amplitude $\beta$ for the transition density or the transition potential. We relate this to the matrix elements $M_\mu$, for $\mu$ = proton ($Z$), neutron ($N$) or isoscalar sum ($A$) by [1]

$$M_\mu=\mu\beta R\langle r\rangle/\pi \tag{1}$$

for a final state of natural parity and multipolarity $L=2$, using $R$ as the midpoint radius $c$ of the ground-state density

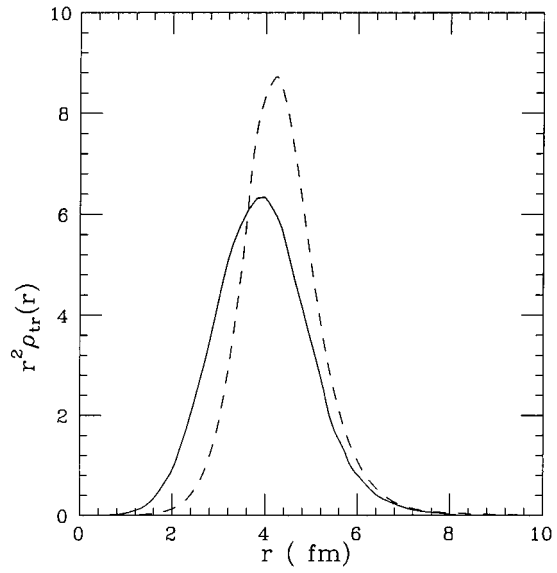


FIG. 3. Transition densities for the vibrational (solid) and microscopic (dashed) models for the first $2^+$ state in $^{52}$Cr are compared, as described in the text, weighted by $r^2$. The integral of these curves gives matrix elements which square to give $B(C2)\uparrow = 672e^2$ fm$^4$. The close similarity of these shapes authorizes our use of the collective model even for a shell-model excitation.

[or optical potential for the distorted-wave Born approximation (DWBA) used below] and $\langle r \rangle$ computed from Woods-Saxon matter distributions to be 3.385 fm.

The transition matrix elements for protons ($M_p$) and neutrons ($M_n$) were taken from a previous pion-scattering experiment for the $2_1^+$ transition [2] but were varied to fit the magnitudes of the $2_3^+$ inelastic cross sections from this experiment, as previous data were not as reliable. The values of $\beta$ and resulting matrix elements are listed in Table I. The $2_1^+$ value for $M_p$ compares favorably with electomagnetic data [5] while the proton matrix element gives a proton (charge) transition rate for the $2_3^+$ state, $B(C2)\uparrow = (18 \pm 6)e^2$ fm$^4$, which also compares well with the value of $12e^2$ fm$^4$ from an average of electromagnetic transitions [6]. We use for the $2^+$ states $B(\mu_2)\uparrow = e^2 M_\mu^2/(2J_i+1)$ from a state of spin $J_i$.

TABLE I. Matrix elements in fm$^2$ and amplitudes $\beta$ for the transitions considered in this work are listed. The results for the pion-induced transitions to the first and third $2^+$ states were obtained through comparison with pion data (this work and Ref. 2) with statistical errors as given. The pion values used for the $2_2^+$ excitations were only those extracted from electromagnetic (EM) measurements [6] where neutron parameters were scaled by $N/Z$. These are bracketed because no acceptable fit to pion data was obtained for this transition. The $\alpha$ scattering $M_0$ was obtained directly from the pion results for the $2_1^+$ state; hence, no errors are reported. Otherwise, the values were from fits to the $\alpha$ data again with statistical errors given.

| | $0^+ \to 2_1^+$ | $0^+ \to 2_2^+$ | $2_1^+ \to 2_2^+$ | $0^+ \to 2_3^+$ |
|---|---|---|---|---|
| $M_p$(EM) | 25.9±0.6 | 1.1±0.2 | 27±3 | 3.5±0.3 |
| $M_p(\pi)$ | 24.2±0.5 | [1.1] | [27] | 4.3±0.7 |
| $M_n(\pi)$ | 21.8±0.5 | [1.3] | [32] | 9.5±0.7 |
| $M_0(\alpha)$ | 46.1 | 0.0 | 33±5 | 12.9±1.3 |
| $\beta_p(\pi)$ | 0.23 | 0.01 | 0.12 | 0.04 |
| $\beta_n(\pi)$ | 0.18 | 0.01 | 0.12 | 0.08 |
| $\beta_0$ | 0.16 | 0.00 | 0.11 | 0.04 |

The seniority shell model fails dramatically to account for the equal cross sections found for $\pi^+$ and $\pi^-$. A purely proton excitation at the delta resonance yields the naive expectation of a $\pi^+$ cross section 9 times greater than that for $\pi^-$. Rather, the symmetry found indicates the proportionate contribution of neutron amplitudes.

The data for the second $2^+$ state, shown in Fig. 2, are clearly not like the diffractive shape for the $2_1^+$ and $2_3^+$ transitions of $^{52}$Cr. This result is not a function of strength alone as there are other weakly excited $2^+$ states with cross sections no stronger than those for this 2.96 MeV peak that do show standard $L=2$ diffraction patterns [1].

In an attempt to reproduce this angular distribution we use a two-step sequential scattering model through the $v = 2$ first $2^+$ state to excite the second $2^+$ state of $v=4$. The proton quadrupole transition strength from the 1.43 MeV state to that at 2.96 MeV is taken from the photon decay data for the higher state [6], with $B(C2)\uparrow = 146e^2$ fm$^4$. The neutron matrix element is scaled by $N/Z$. This purely second-order calculation yields the dotted curve compared to the $2_2^+$ data in Fig. 2.

There is a small direct photon transition from the 2.96 MeV state to the ground state, corresponding to $B(C2)\uparrow = 1.3e^2$ fm$^4$ [6]. The weakest $2^+$ state seen in electron scattering from $^{52}$Cr has $B(C2)\uparrow = 16e^2$ fm$^4$ [7]. We use a direct matrix element $M_p = 1.1$ fm$^2$, and scale the neutron amplitude by the total number of neutrons and protons in $^{52}$Cr to obtain $M_n = 1.3$ fm$^2$. The dotted curve in the bottom panel of Fig. 2 is a pure two-step calculation while the solid and dashed curves show the influence inclusion of interfering direct amplitudes has on the calculation for the 2.96 MeV cross section. The solid curve shows the prediction with the same relative sign for the first- and second-order matrix elements for neutrons and protons, and with the positive sign between amplitudes for neutrons and protons. This maintains the isoscalar symmetry expected from pion scattering to low-lying states [1]. An opposite choice of the relative sign between the two-step and one-step amplitudes yields the dashed curve for the $2_2^+$ cross section. The small one-step amplitudes lead to only small differences in the shapes of the two predictions, but we find that the opposite sign causes a destructive interference of about a factor of 3 in the magnitudes. It must be emphasized that this calculation for the $2_2^+$ state includes no free parameters aside from this sign. The form factor shapes were determined by the elastic scattering, the first $2^+$ cross section was taken to fit those data, and the transitions to the $2_2^+$ state itself were obtained from electromagnetic data. The mixed and purely two-step computed cross sections give roughly the correct magnitude for the $2_2^+$ transition, but fail to account for the shape observed. (If we allow all of the $\beta_\mu$ parameters to be free, reproduction of the shape can still not be made).

## III. $\alpha$ PARTICLE SCATTERING

The only $\alpha$-particle-scattering data we were able to find for the weak 2.96 MeV peak in $^{52}$Cr were at 42 MeV,

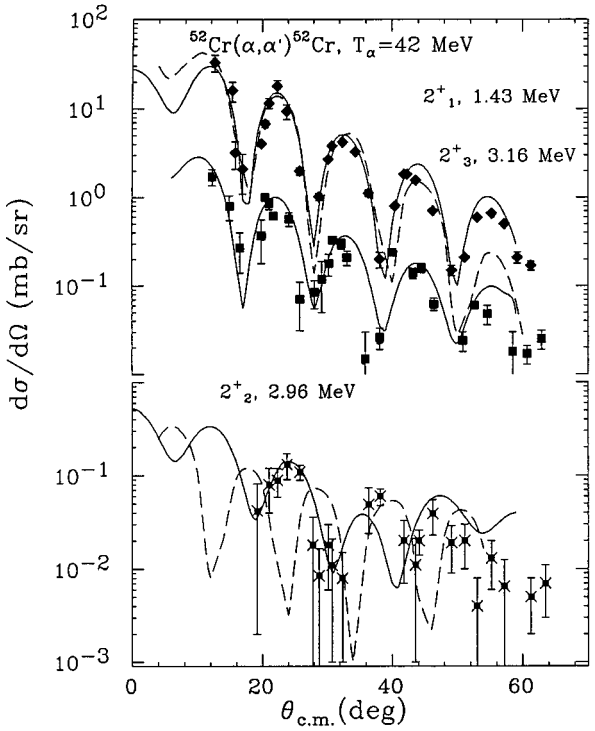


FIG. 4. Inelastic scattering of 42 MeV $\alpha$ particles to the first three $2^+$ states of $^{52}$Cr yields data compared here to first-order and purely second-order DWBA calculations, using the deformations or matrix elements listed in Table I. These are shown by solid lines. The dashed curve for the $2^+_1$ state gives the Fraunhofer calculation, described in the text, which is is also successful in reproducing the shape and magnitude of these data. For the $2^+_2$ transition, the dashed curve is proportional to $J_1^2(x)$ and matches the observed shape only at the large angles.

using silicon particle detectors [15]. The resolution of 105 keV was sufficient to resolve the state cleanly, and a companion spectrum taken with the same target using a magnetic spectrograph with 60 keV resolution observed the 2.96 MeV state with the same relative strength. The target was isotopically enriched to 99.9%. The general method used for these data has been reported for other nuclear targets [16]. The cross sections for the first and second $2^+$ states of $^{52}$Cr are shown in Fig. 4.

First- and second-order distorted-wave Born approximation (DWBA) calculations were carried out with the coupled-channels code CHUCK2 [17]. The optical-model parameters were taken from fits to elastic scattering from $^{52}$Cr at 42 MeV [18]. The transition potential was taken to be the first derivative of this optical potential, with deformation parameters listed in Table I. For the first $2^+$ state of $^{52}$Cr, the solid curve in Fig. 4 shows the cross section predicted using an isoscalar matrix element $M_0$ as the sum of the values used for the pion scattering (the dashed curve represents a Fraunhofer calculation to be discussed later). This is clearly successful, accounting for the shape and the magnitude of the $\alpha$ scattering data with no new parameters.

The same model applied to the 3.16 MeV $2^+_3$ transition gives the fit shown in Fig. 4 with $\beta = 0.04$, which yields $M_0 = 12.9$ fm$^2$. This is near the sum of $M_n + M_p = 13.8$ fm$^2$ from the pion work. The diffractive shape of the $\alpha$ scattering angular distribution is adequately fit.

The $\alpha$ scattering cross sections to the second $2^+$ state of $^{52}$Cr are, however, far from the simple diffractive shape. Use of the sum of the proton and neutron matrix elements from the first to the second $2^+$ state gave cross sections far in excess of what was seen for $\alpha$ scattering, as seen by the values of $\beta$ listed in Table I. The solid curve compared to the 2.96 MeV data in Fig. 4 uses the same matrix elements as for the pions to the 1.43 MeV state, as in comparison to the data above in Fig. 4, but uses an isoscalar matrix element of only $M_0 = 32.5$ fm$^2$ for the second step to the 2.96 MeV state, with $\beta_{12} = 0.156$. This is a smaller isoscalar matrix element than the value of 59 fm$^2$ found from the pion analysis. Inclusion of a direct matrix element $M_0 = 2.4$ fm$^2$ from the ground state to the 2.96 MeV state made changes in the shape and magnitude of this curve only at the largest angles, using either relative sign.

The pure two-step calculation accounts very well for the shape of the $2^+_2$ $\alpha$ scattering data, as expected for a $v=4$ excitation. If only the proton matrix element, not the isoscalar sum, from the pion fit were used to form $M_0$, the two-step prediction would be nearly in agreement with the $\alpha$ particle data. That would be consistent with the seniority shell model for the second transition, from a $v=2$ proton state to one of $v=4$.

## IV. DIFFRACTION MODEL

The sharply diffractive angular distributions for the first $2^+$ state using spin-zero pions and $\alpha$ particles invite use

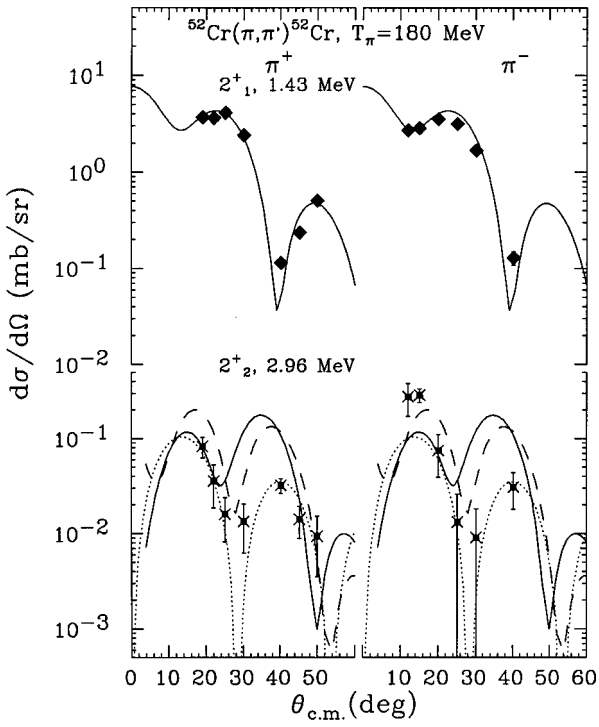


FIG. 5. The 180 MeV pion data are compared to Fraunhofer calculations, using the parameters listed in the text and Eq. (2). Only a first-order ($A=1$) curve is used for the $2^+_1$ transition. The solid curve for the 2.96 MeV data uses the best fit using Eq. (2), with $A=-0.11$. The dashed curve uses $A=0$ for a purely two-step mechanism. Neither of these matches the data as well as the dotted curve which is undamped and proportional only to $J_1(x)^2$.

of the Fraunhofer model, diffracting the beam around a black disk. This model can be extended to second order [19,20]. The radius of the black disk, $R$, is taken from the minima of the $2_1^+$ angular distributions, and the beam center-of-mass wave number is $k$, using the argument $x=2kR\sin\theta/2$. This is the most accurate approximation for the shadow cast by the disk at a center-of-mass scattering angle $\theta$. A trapezoidal transition from absorption to transmission occurs over a distance $\Delta$, damping the prediction at larger angles by the factor $D=\mathrm{abs}2J_1(y)/y$ for each single scattering amplitude, with $y=2k\Delta\sin\theta/2$. Here the $J_{0,1,2}$ represent Bessel functions of the given order. The overall magnitudes of the cross sections are given by an amplitude $\beta$, as also used in the coupled-channels calculations. If we take the $2_2^+$ state to be the two-phonon vibrational state, the two-step path to it is determined by the magnitude of the $2_1^+$ cross sections for both beams. We also allow an amplitude $A$ for the $2_2^+$ state to mix with an amplitude $\sqrt{1-A^2}$ for a direct excitation ($A=1$ for pure one step), with the same value of $\beta$ as for the first $2^+$ state.

The expression that results for the second $2^+$ state Fraunhofer cross section is then

$$\frac{d\sigma}{d\Omega_{\mathrm{c.m.}}}=\frac{(kR_0)^2(\beta R_0)^2}{4\pi}\left[\frac{AD}{2}J_0(x)+\sqrt{1-A^2}D^2\frac{k\beta R_0}{7}\sqrt{\frac{5}{16\pi}}[J_0(x)-xJ_1(x)]\right]^2$$
$$+\frac{[2(kR_0)^2(\beta R_0)]^2}{4\pi}\left[\sqrt{\frac{3}{8}}ADJ_2(x)+\sqrt{1-A^2}D^2\frac{k\beta R_0}{7}\sqrt{\frac{15}{32\pi}}[-J_2(x)-xJ_1(x)]\right]^2. \quad (2)$$

Curves for the $2_1^+$ state from pion scattering are shown in Fig. 5, using the parameters obtained from these $2_1^+$ data ($R=5.33$ fm, $\Delta=2.0$ fm, and $\beta R=0.80$ fm) and the expression above with $A=1$. The isoscalar matrix element obtained from this value of $\beta R$ is 44.8 fm$^2$, very near that obtained by distorted wave methods, 46.0 fm$^2$. Also in Fig. 5 are the Fraunhofer predictions for the $2_2^+$ state, using the full expression, with a fit resulting from a search on the parameter $A$ over the data sets for both pion signs. We find some improvement from this search using $A=-0.11$ (solid curve) but the dashed lines shown with a purely two-step calculation ($A=0$) differ little from the optimum, and both fail to give a good fit. Also shown is the shape (dotted) using an undamped form proportional to $J_1^2(x)$ alone, which does account for the shapes found.

The diffraction model with $R=6.63$ fm and $\Delta=1.25$ fm, found to fit the elastic data of [15], is used to also fit the $2_1^+$ data for $\alpha$ particle scattering in Fig. 4. The fit shown by the dashed line yielded $\beta=0.16$, exactly as found by the DWBA. The fit is excellent in shape and magnitude.

Since it was found to be successful for the $2_2^+$ pion data, a simple undamped $J_1^2(x)$ shape is also shown against the $\alpha$ scattering data for the $2_2^+$ state in Fig. 4, but with not much agreement.

## V. DISCUSSION AND CONCLUSIONS

The first striking thing we note from the pion data is the isospin symmetry, with nearly equal $\pi^+$ and $\pi^-$ cross sections or proton and neutron matrix elements for all three $2^+$ states of $^{52}$Cr considered. Other states of $^{52}$Cr reported in [2] also exhibit this symmetry. The general systematics lead one to expect this for the $2_1^+$ state, but the shell model for a seniority-4 description of the $2_2^+$ state is so compelling that the new experiment was carried out to examine the anticipated protonlike excitation.

A similar case of four neutrons from a closed shell is found for $^{44}$Ca. Pion scattering to the $2_2^+$ state of $^{44}$Ca at 2.66 MeV shows a clear single-excitation diffraction pattern, in contrast to the case of $^{52}$Cr [21]. The $^{44}$Ca data are also charge symmetric. The structure of the two $2_2^+$ states is evidently greatly different, as shown by the direct electromagnetic excitations from the ground states, stronger by a factor of 80 in the case of $^{44}$Ca [22]. This allows the greater one-step strength seen for $^{44}$Ca by the pion scattering.

Another appropriate comparison of the $^{52}$Cr $2_2^+$ data is to the ''reversal'' states seen in pion scattering [23]. These are higher $2^+$ states, often the second, that show clear $L=2$ angular distributions but without the charge symmetry so widely noted. The reversal of these $2^+$ states arises from there being two dominant shell-model amplitudes, mixing with a constructive sign for the lowest $2^+$ state and destructively for the other. For instance, a $p$-shell excitation could provide a second amplitude to give this effect in $^{52}$Cr. A proton stripping experiment, however, finds no excitation of the 2.96 MeV state of $^{52}$Cr from the $v=1$ ground state of $^{51}$V, for either $f$-shell or $p$-shell strength [24].

Although our study of the $v=4$ state could be enhanced by comparisons to pion double charge exchange, there are no data with similar beam energies or targets for final $2^+$ states in DCX. Ground-state (non-DIAS) DCX cross sections near our target mass give cross sections of about 50 nb/sr. Inelastic scattering to a $v=4$ state will be stronger than for DCX because the scattering can proceed by the stronger isoscalar couplings not available to DCX.

We also note that the simple ratios of $2_2^+$ to $2_1^+$ cross sections are much greater for pion scattering than for $\alpha$ particle scattering. Our calculations reproduced this effect by decreasing the second step amplitude for $\alpha$ scattering from the $2_1^+$ state. A greater pion cross section could be a sign of some two-step path not available to the $\alpha$ particles. Since the pion experiment was carried out at the 3-3 resonance, several such channels could be postulated.

Furthermore, the pion data for the $2_2^+$ state can be fitted to

a simple $J_1^2$ squared shape, not anticipated for a transition from a $0^+$ to a $2^+$ state. A similar case was found for charge exchange of strongly absorbed particles in the ($^3$He,$t$) reaction from $0^+$ ground states to $0^+$ final states, the so-called anti-analog states [25]. An explanation in terms of two interfering $L=0$ amplitudes to form an $L=1$ pattern has been presented [26].

The simple $(f_{7/2})^n$ seniority shell model clearly failed to account for the pion data, in either shape or magnitude. This model did successfully give the purely two-step $\alpha$-particle-scattering angular pattern, but the magnitude was not that expected from electromagnetic results and an isoscalar collective symmetry [27]. The seniority shell model is broken by the inclusion of $p$-shell nucleons, and this extension does account better for the observables in $^{52}$Cr [28]. There is evidently no $p$-shell stripping to the 2.96 Mev $2_2^+$ state of $^{52}$Cr [24], and so the higher shell nucleons must remain in some configuration much more complex than the other low-lying states. This $2_2^+$ state, examined here by pion and $\alpha$ particle scattering, is in several ways a counterexample to the usual successes with models. Our simple structure and reaction models were not able to give a fully consistent set of results to agree with the data, and the explanation of this puzzling case remains open.

## ACKNOWLEDGMENTS

This work was in part supported by the U.S. Department of Energy, under Grant No. DE-FG02-86ER40269, and the National Science Foundation. We would like to thank G. Liu, A. Petit, A. Williams, and R. Winter for their assistance in data collecting and analysis.

[1] R. J. Peterson, Phys. Rev. C **48**, 1128 (1993).
[2] D. S. Oakley *et al.*, Phys. Rev. C **35**, 1392 (1987).
[3] I. Talmi, Phys. Rev. **126**, 1096 (1962).
[4] T. Komoda, Nucl. Phys. **51**, 234 (1964).
[5] P. M. Endt, At. Data Nucl. Data Tables **23**, 547 (1979).
[6] H. Junde, H. Dailing, S. Huibin, Y. Janming, and H. Baohua, Nucl. Data Sheets **58**, 677 (1989).
[7] J. W. Lightbody *et al.*, Phys. Rev. C **27**, 113 (1983).
[8] D. S. Oakley *et al.*, Phys. Rev. C **44**, 2058 (1991).
[9] L. Peker, Nucl. Data Sheets **43**, 481 (1984).
[10] M. N. Rao, J. Rapaport, A. Sperduto, and D. L. Smith, Nucl. Phys. **121**, 1 (1968); A. MacGregor and G. Brown, *ibid.* **88**, 385 (1966).
[11] E. Rost, computer code CHOPIN, University of Colorado, 1979 (unpublished); M. Kagarlis, Los Alamos Report No. LA 12443-T, 1993.
[12] R. A. Eisenstein and G. A. Miller, computer code DWPI, Comput. Phys. Commun. **11**, 95 (1976).
[13] G. Rowe, M. Saloman, and R. H. Landau, Phys. Rev. C **18**, 584 (1978).
[14] R. J. Peterson, Ann. Phys. (N.Y.) **65**, 125 (1971).
[15] R. J. Peterson, Ph.D. thesis, University of Washington, 1966 (unpublished).
[16] R. J. Peterson, Phys. Rev. 172, 1098 (1968).
[17] P. D. Kunz, computer code CHUCK, a coupled-channels reaction, University of Colorado, 1977 (unpublished).
[18] B. Fernandez and J. S. Blair, Phys. Rev. C **1**, 523 (1970).
[19] J. S. Blair, in *Lectures in Theoretical Physics*, edited by P. D. Kunz, D. A. Lind, and W. E. Brittin (University of Colorado Press, Boulder, 1966).
[20] N. Austern and J. S. Blair, Ann. Phys. (N.Y.) **33**, 15 (1965).
[21] S. Mordechai *et al.*, Phys. Rev. C **36**, 1950 (1987).
[22] P. M. Endt, Nucl. Phys. **A521**, 1 (1990).
[23] V. R. Brown, A. M. Bernstein, and V. A. Madsen, Phys. Lett. **164B**, 217 (1985).
[24] F. Pellegrini, I. Filosofo, M. I. El Zaiki, and I. Gabrielli, Phys. Rev. C **8**, 1547 (1973); D. L. Watson and G. Brown, Nucl. Phys. **A296**, 1 (1978).
[25] R. A. Hinrichs, R. Sherr, G. M. Crawley, and I. Proctor, Phys. Rev. Lett. **25**, 829 (1972).
[26] R. Schaeffer and G. F. Bertsch, Phys. Lett. **38B**, 159 (1972).
[27] P. Van Isacker, M. A. Nagarajan, and D. D. Warner, Phys. Rev. C **48**, 1466 (1993).
[28] N. Auerbach, Phys. Lett. **24B**, 260 (1967).